31 August 2023
ciara.losel@cern.ch

Analysing the robustness of the R2E MCWG BLM monitoring code

Ciara Losel
Supervisors: Auriane Canesse, Giuseppe Lerner

Keywords: Beam Loss Monitor, total ionising dose, R2E, MCWG

Summary

The Radiation To Electronics (R2E) project at CERN focuses on safeguarding electronic systems exposed to radiation by particle accelerators. The Monitoring and Calculation Working Group (MCWG), a component of R2E, oversees radiation assessment and develops strategies to counteract potential effects. The Total Ionising Dose (TID) measurements recorded by these devices are used to establish radiation levels in different areas of the Large Hadron Collider (LHC), which is monitored using the BLM monitoring code. This report demonstrates the analysis of the robustness of this current code system by compar- ing different design choices and analysing the impact of using the implementation that is currently in place.

Contents

1 Introduction

For my summer student project I worked within the R2E MCWG group to analyse the robustness of the BLM monitoring code that is currently in use. The Radiation To Electronics (R2E) project at CERN focuses on safeguarding electronic systems exposed to radiation by particle accelerators. The Monitoring and Calculation Working Group (MCWG), a component of R2E, oversees radiation assessment and develops strategies to counteract potential effects.

MCWG utilises devices like Beam Loss Monitors (BLMs) to monitor radiation levels. BLMs are devices that detect particle losses within accelerators, ensuring safety by triggering protective measures and providing measurements of Total Ionising Dose (TID) for radiation monitoring. The TID measurements recorded by these devices are used to establish radiation levels in different areas of the Large Hadron Collider (LHC), which is monitored using the BLM monitoring code.

My project involved analysing the robustness of this current code system by comparing different design choices and analysing the impact of using the implementation that is currently in place.

2 Background

2.1 MCWG BLM analysis

The emission of radiation by the accelerators at CERN can impact the operational integrity of nearby electronic systems. The R2E project is dedicated to safeguarding the functionality of these electronics. This is achieved through an approach encompassing monitoring, calculation, mitigation, and the development of radiation-resistant systems.

The Monitoring and Calculation Work Group (MCWG) primarily focuses on overseeing the monitoring and calculation aspects of the R2E project. MCWG monitors several physical quantities: the Total Ionising Dose (TID) which is measured in Grays (Gy) and several particle fluences. The TID corresponds to the energy deposited by charged particles in a given material through ionisation. Fluence, on the other hand, is the number of particles going through a given surface. In the LHC, TID is measured with 3 types of detectors: Beam Loss Monitors (BLMs), optical fibers, and Radmons [1].

Beam Loss Monitors are ionization chambers strategically positioned to measure radiation levels at their specific locations. These devices are fixed to the outside of the LHC magnet cryostats at intervals and can be situated alongside either beam 1, beam 2, or in the central region. There are approximately 4000 BLMs distributed across the LHC. Their primary purpose is to ensure machine protection, as the detection of radiative losses surpassing a predetermined BLM threshold triggers a beam dump to avoid damage from beam machine interactions. In addition to this primary role, MCWG leverages BLMs for secondary monitoring purposes, utilizing them to measure radiation levels in the CERN accelerator complex by integrating the measured dose rate to compute the total TID received over relevant time periods.

This report pertains to the current BLM monitoring code developed by [2]. The functioning of this code is based on segmenting operational runs into beam intervals, defined as periods when at least one beam is present, which may not necessarily align with fill start or end times. The TID at each BLM is integrated over these intervals, referred to as BLM intervals. Alongside the integrated dose rate, the dose rate preceding and following the interval is measured to establish baseline dose rates in the absence of beam activity. These baseline measurements are termed offsets and are computed by averaging measured dose rates over a five-minute duration. The offset before the interval is termed the pre-offset, while the offset after is the post-offset. These offset values are then scaled to the BLM interval duration and subtracted from the TID measured during the interval to correct for background radiation levels. The data storage format in the analysis database is illustrated in Figure 1.

BLM name	Start time	End time	TID	TID corrected using pre-offset	TID corrected using post-offset	Pre-offset	Post-offset
BLMQI.25L6.B1E10_MQ	2023-06-06 01:46:11	2023-06-06 02:28:35	0.000454	0.000000	0.000006	1.786e-07	1.761e-07
BLMQI.27L3.B1I30_MQ	2023-05-19 13:28:38	2023-05-19 13:45:27	0.000109	1.792e-07	1.792e-07	1.308e-07	1.308e-07

Figure 1: BLM interval data as seen in database.

In low radiation areas, marginal fluctuations in measured dose can lead to baseline levels slightly exceeding the TID recorded within BLM intervals. Consequently, corrective measures are applied, resulting in negative TID values. Recognizing the impossibility of negative doses, these values are adjusted to zero. This non-negative adjustment can be observed in Figure 1, where one TID measurement after pre-offset removal equates to zero.

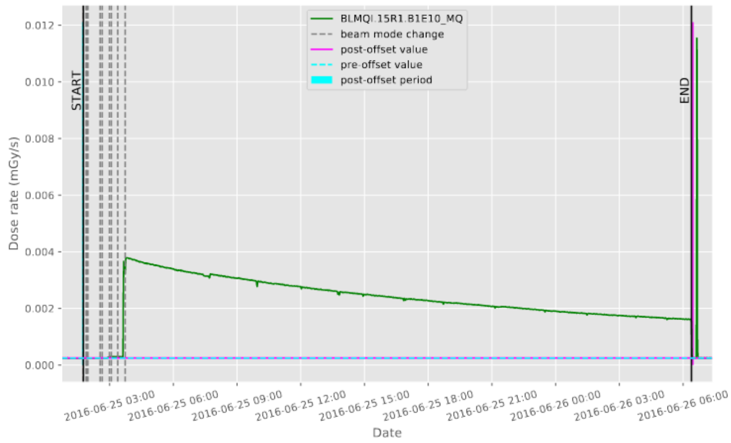

Figure 2: One BLM interval with pre-offset and post-offset. Figure 16 from [2].

In the calculation process, selecting the appropriate offset method is pivotal, given the existence of two distinct methods. The work by [2] discusses the occurrence of significant dose spikes after fills due to BLM device resets, which generate an overestimation of the baseline levels. To address this, an approach is implemented to exclude offset intervals coinciding with these spikes, identified as dose fluctuations. However, considering that these reset spikes consistently occur post-fill, pre-offset removal is preferred to avert the propagation of these spikes into measurements. Instances still arise where the post-offset is essential. For instance, in cases of closely spaced beam intervals, insufficient time exists between them to calculate a five-minute offset. In such scenarios, the nearest offset interval measurement is used, which could be either the post-offset or the most recent pre-offset measurement. The presence of post-offsets remains essential to address this.

This project report presents the outcomes of an analysis examining the robustness of the current system by comparing the design choices discussed above.

2.2 Offset measurements and their importance

This report details the analysis of certain design choices made during the development of the current BLM monitoring code presented by [2]. To perform this analysis, the measurements for raw TID, offsets and corrected TIDs from BLM intervals were used. It's important to establish the relationship of these measurements before using them to compare difference implementations.

In Figure 3, we can see how the total TID measured in 2022 for each BLM varies across the LHC in Point 5. We can see high total dose occurring where the CMS experiment is. Far away from the experiment, the BLMs measure relatively low doses throughout 2022.

Now let's consider the offset measurements. In 4a, we can see how the offset measurements summed over a year certainly don't have any relationship with the summed raw TID. Now looking at how these offset measurements compare against the time they were measured at

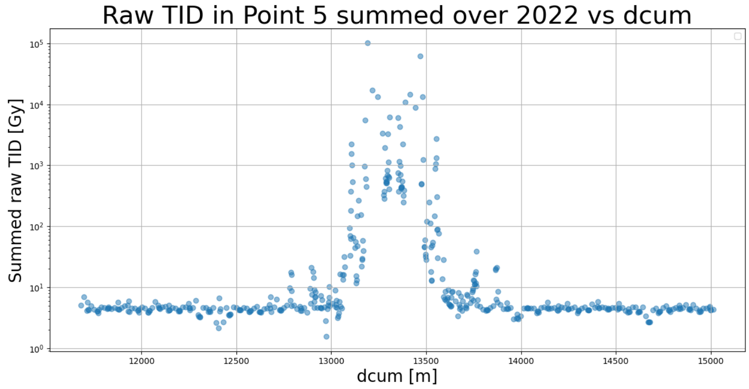

Figure 3: Total TID measured by each BLM over 2022.

in Figure 4b, we can see step-like progressions at certain times. Colleagues from the Beam Instrumentation group provided insight into this by explaining the safeguarding mechanism involving a consistent current being supplied to the input. The variation of the baseline levels show the necessity of computing its value at every fill.

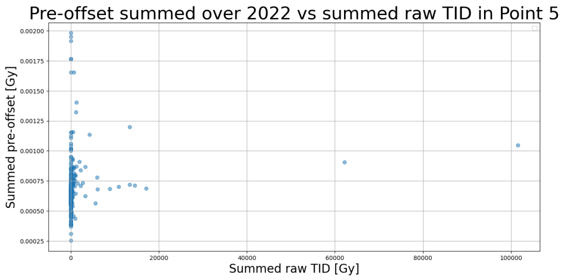

(a) Total pre-offset measured in 2022 against the total TID measured in 2022 for each BLM.

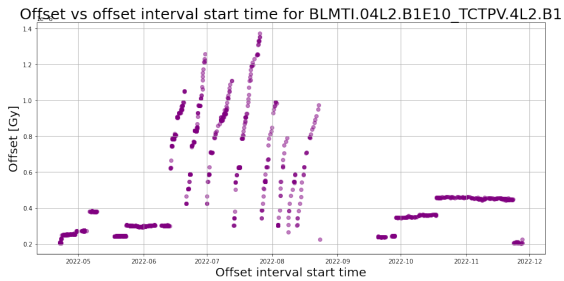

(b) Offset against time offset was measured at for one BLM.

Figure 4

One would expect all the offset measurements to be fairly stable, since they are all measured when no beam is present. However, these plots show that this is in fact not the case, and that they instead vary across different fills. Hence, these offset values can't be predicted and so it is important that they are measured for every beam interval.

3 Data selection

As detailed in Section 2, the LHC accommodates approximately 4000 BLMs, but processing them all would be too time consuming. A representative BLM sample was chosen: BLMs around P5 from cell 14L5 to 14R5. This area hosts the CMS experiment, thereby offering a hub of notable activities. The analysis was further limited to data from the year 2022, ensuring a reasonable amount of data to work with.

Recalling that each BLM has a compilation of recorded BLM intervals, the exploration of individual BLM results for every BLM was unreasonable, and so a representative sample of BLMs was chosen to investigate. The sample encompassed BLMs with markedly low (0-200 Gy), high (800-1000 Gy), and medium (400-600 Gy) typical annual dose measurements. The following BLMs were included in this sample, as illustrated in the table below.

BLM name	**Dose (Gy)**
BLMEI.06R5.B1E10_XRP.E6R5.B1	879
BLMTI.05L3.B2E10_TCLA.A5L3.B2	15
BLMQI.01R5.B2I20_MQXA	310
BLMQI.03L2.B2I30_MQXA	377

4 Results

Section 2 provides an exposition of the various design considerations undertaken during the implementation of the present BLM monitoring code. In order to assess the code's robustness, a comparison was conducted involving three specific design choices and their alternative approaches.

Firstly, an investigation was undertaken to compare two different dose rate variables. The comparison involved contrasting the effects of using the existing dose rate variable, known as running sum 12, a higher resolution variable known as running sum 9. Detailed examination of the distinctions between these variables and the comparison results are addressed more comprehensively in Section 4.1.

Secondly, it was examined whether TID values could become negative after removing their offsets, compared to the current method of making negative values zero. This assessment and its results are covered in Section 2 4.2.

Lastly, the investigation encompassed an evaluation of the implications stemming from the selection of the pre-offset versus the post-offset. This inquiry sought to assess the efficacy of the current offset selection methodology. The outcomes arising from this comparison are elaborated upon in Section 4.3.

4.1 Running sum 9 versus running sum 12

This section discusses the two dose rate variables running sum 9 and running sum 12. The current method for monitoring radiation uses the longest running sum 12 which averages the dose rate over 83.89 seconds. How the two running sums differ when measuring dose rate during one beam interval can be seen in Figure 5. It's important to identify any large discrepancies between these two data sets, so that one can be sure that running sum 12 is an appropriate time resolution for the BLM monitoring code.

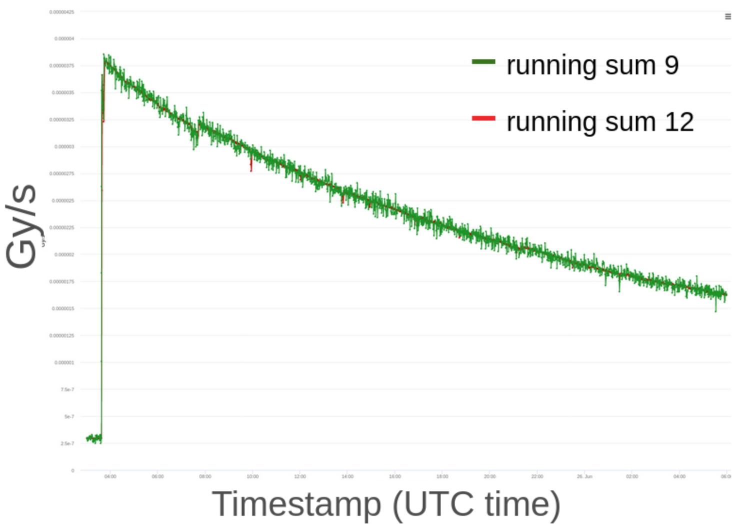

Figure 5: TID for one beam interval showing running sum 9 and 12.

4.1.1 Summed data across 2022 per BLM

In Figure 6 one can see how the total raw TID in 2022 measured for each BLM in Point 5 varies with the position in the LHC using running sum 9 and running sum 12. The ratio plot shows how different the running sums are. From this, one can see that using running sum 9 produces slightly larger total TIDs than running sum 12.

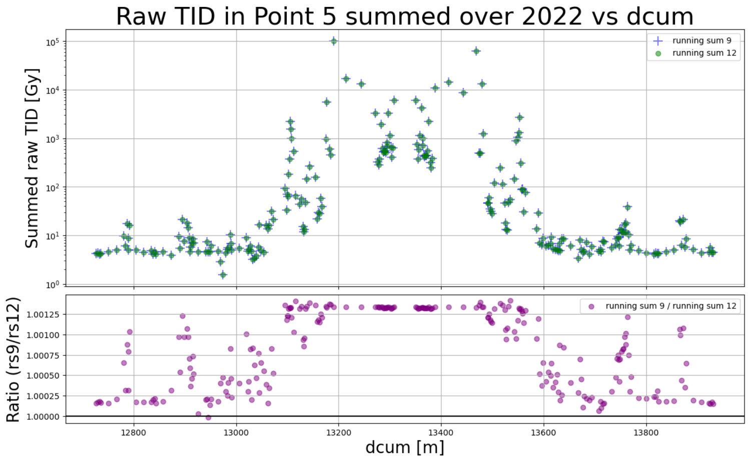

Figure 6: Total TID measured for each BLM in 2022 against dcum.

There is also an interesting plateau in the ratio occurring at high dose BLMs. The fact that this plateau occurs at a ratio of 1.00125 is an interesting feature and requires further analysis.

Figure 7 shows the same type of plot, but for TID values corrected using the pre-offset. In contrast, the ratio shows that the use of running sum 9 now produces slightly smaller values than using running sum 12. Also, the larger differences occur for high dose BLMs. The same kind of behaviour is seen when using the pre-offset instead.

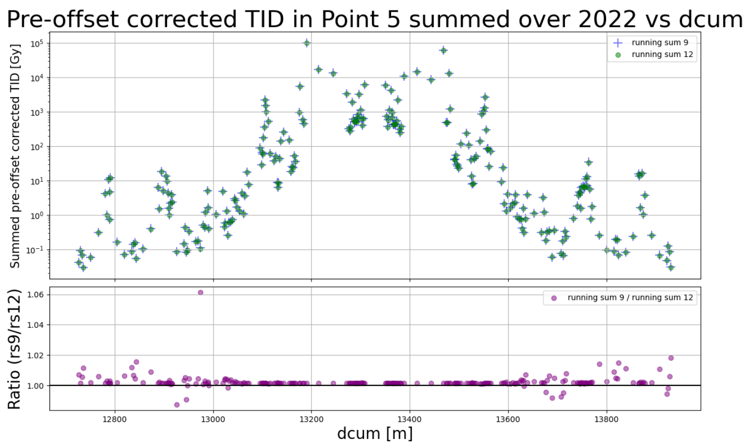

Figure 7: Total pre-offset corrected TID measured for each BLM in 2022 against dcum.

4.1.2 Single BLM analysis

This section presents the results from comparing running sum 9 and 12 for just one BLM, specifically BLMEI.06R5.B1E10_XRP.E6R5.B1.

Figure 8 shows the difference between TIDs measured using running sum 9 and running sum 9. All these differences are positive, hence running sum 9 is always larger. This is in support of what was seen for in Figure 6, in which running sum 9 generally gave larger values then running sum 12 when comaparing TID values.

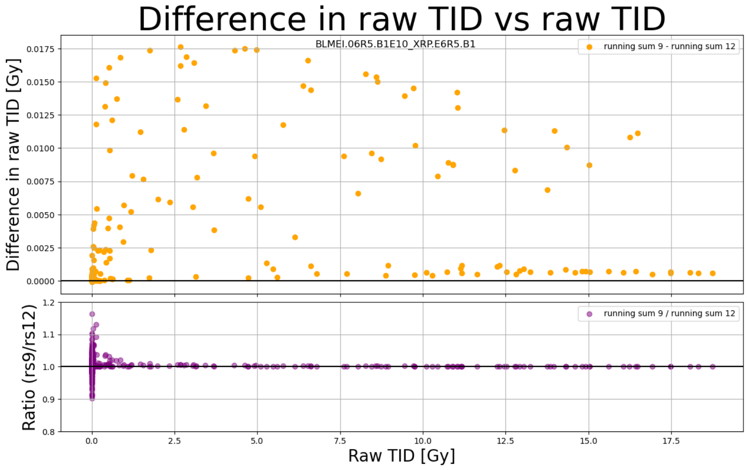

Figure 8: Difference between TID measured by running sum 9 and TID measured by running sum 12 against TID.

However, the contrasting relationship is again seen for both offset measurements, in which running sum 12 is generally larger than running sum 9, as seen in Figure 9. In fact, the difference between the two running sums is still small, being 5% in most bad cases, but 20% for one particularly larger outlier, as shown in Figure 9b. This exaggeration is clearly shown in Figure 10, showing the offset measurements and the time they were measured at separately for the pre-offset and post-offset. One can see lots of points on the right, showing the post-offset, for which the offsets are not the same for both running sums.

Figure 11 shows the dose rate level for one post-offset interval and one pre-offset interval. The green line represents running sum 9 and the red line represents running sum 12. One can see from this Figure that the pre-offset interval measures a constant dose rate level for both running sums, whereas the post-offset interval records a decreasing trend in radiation for both running sums. This was found to occur for many post-offset intervals. This suggests that, in general, the post-offsets are larger than their respective pre-offsets, and this is discussed further in Section 4.3. More importantly for the discussion of running sums, the post-offset measured by running sum 9 has a curve that sits higher than running sum 12, and this is what is causing the post-offset measurements by running sum 12 to be larger than those for running sum 9. One can deduce that, for these decreasing trends in radiation, running sum 12 overestimates the radiation levels.

Since post-offset measurements are taken after a beam interval, that is, there is no beam active, one would expect the post-offset to be a constant measurement of background radiation. However, Figure 11 implies that the dose rate levels measured during a post-offset

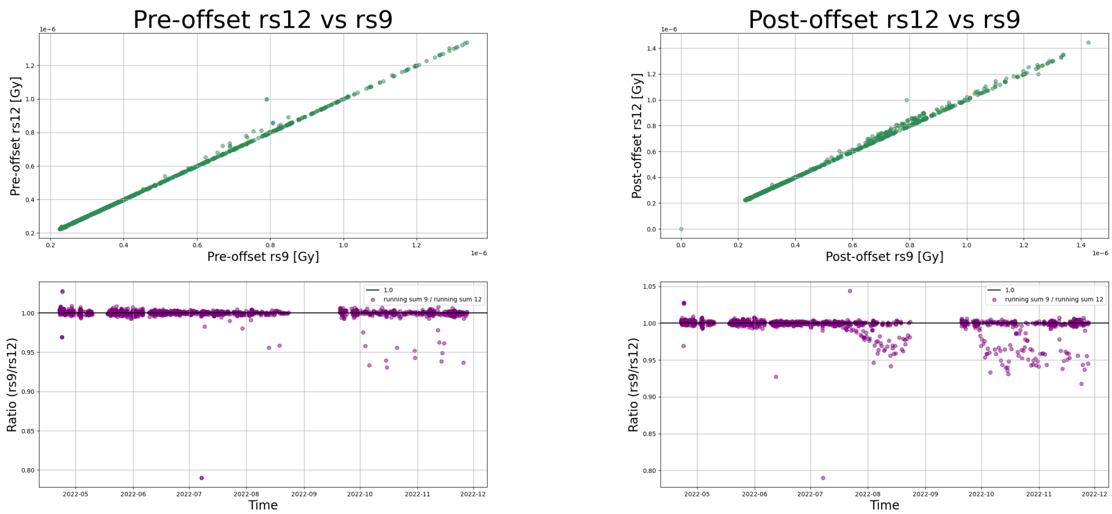

(a) Pre-offset measured by running sum 12 against pre-offset measured by running sum 9 above. Ratio against time below.

(b) Post-offset measured by running sum 12 against post-offset measured by running sum 9 above. Ratio against time below.

Figure 9

interval are actually influenced by some other factor. This could be due to material activation, that is slowly decreasing over time.

4.2 Negative TID correction

It was discussed in Section 2 how the offset-removal may cause some corrected TIDs to be negative, and since this is impossible, these negative values are made equal to 0 in the current analysis software version. The effect of this correction is that we stabilise the fluctuation in the offset measurements, however, this comes at the price of a bias.

It's important to quantify the bias, particularly long-term. That is, when we look at

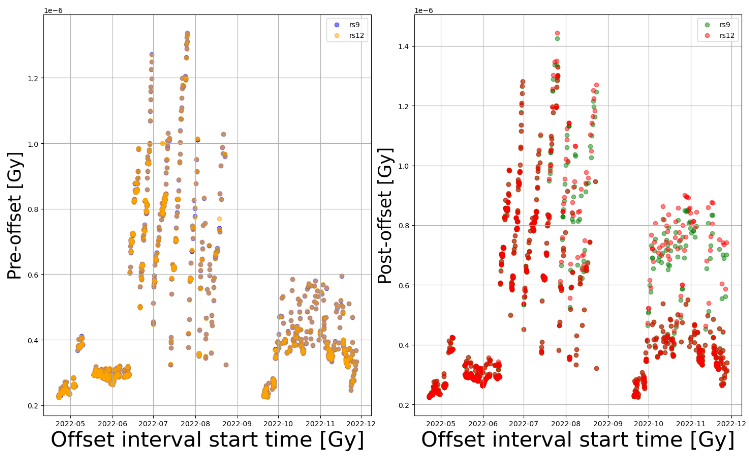

Figure 10: Offsets against the time they were measured at.

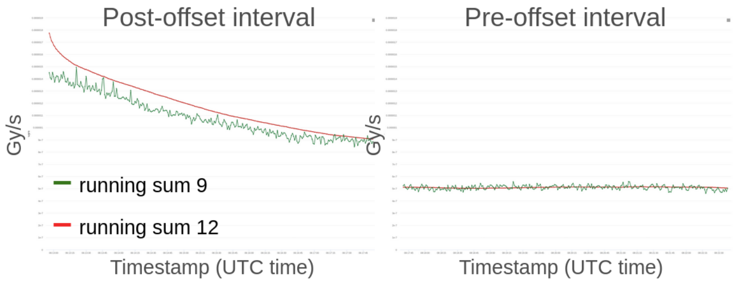

Figure 11: Dose rate measured by BLMEI.06R5.B1E10_XRP.E6R5.B1 during a given post and pre offset time interval.

large intervals of time, does this zero-correction method propagate into the data. We can check this by comparing the summed corrected TIDs that are allowed to be negative when the offset is removed and the summed corrected TIDs that are made equal to zero. Any bias will represent itself as any significant discrepancies in these two data sets.

Figure 12 shows the total TID corrected with the pre-offset measured in 2022 for each BLM. It shows these total TIDs when there are no negative corrected TIDs and when negative corrected TIDs are allowed.

One might expect the total TID for each BLM using the negative data to be much smaller than using the non-negative data. The ratio plot shows that the two data sets are quite similar, however, it's important to note that the y-axis for this comparison is much larger than that for the running sum 9 and 12 comparison. There are several outliers in this figure which show a 50% difference between the two data sets which is significant.

There are three points at which the ratio is actually negative. This must mean that, for these BLMs, there are small negative corrected TID measurements over even smaller positive values causing the total TID in these three BLMs for 2022 to be negative. An interesting feature is that these three outliers occur at BLMs experiencing low doses.

4.3 Pre-offset versus post-offset

Comparing the pre-offset and the post-offset and the effects of using the two different methods is important because it could provide insight into the effectiveness and reliability of the current solution for selecting an offset interval to remove.

If the pre-offset and post-offset values are similar, this indicates that the baseline radiation remains stable during fills. However, as we've seen in Section 4.1, this does not tend to be the case and this Section will confirm this. The behaviour of these two offsets will allow us to potentially identify why they differ.

4.3.1 Summed data across 2022 per BLM

Figure 13 shows the total corrected TID for 2022 for each BLM. It shows clear differences between using the pre-offset and the post-offset at BLMs experiencing low dose rate levels. The difference between using the pre-offset and the post-offset is diminished at high dose rates, since the values are so much larger.

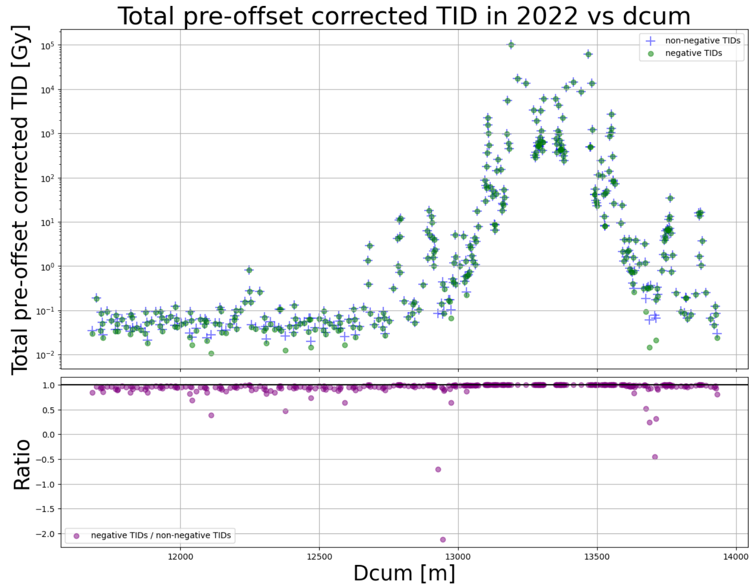

Figure 12: Total pre-offset corrected TID measured per BLM over 2022 against dcum for negative and non-negative TIDs. Note that in the top figure, negative values do exist but are not shown.

Looking at the actual offset measurements, Figure 14 shows the total offset measured across 2022 for each BLM. This shows that the difference between both offset methods is actually relatively small for BLMs measuring low dose rates, but that the difference gets much larger as the radiation increases. The ratio plot shows that the post-offset is larger than the pre-offset when the dose rate is larger.

This result is expected due to the discussion in Section 4.1.2 when looking at Figure 11, when it was shown that post-offsets typically involve a decreasing trend in radiation, whereas pre-offsets typically measure a constant level of radiation. This relationship is reflected in Figure 14, showing that the difference between the two offsets is significant even when summing the radiation for the entire year.

4.3.2 Low dose BLM analysis

In this section, the comparison of the pre-offset and post-offset measurements for BLMTI.05L3.B2E10_TCLA.A5L3.B2 is discussed. This BLM is not positioned in Point 5, however it showed some interesting results, which are now discussed.

Figure 15 shows the pre-offset against the post-offset for every BLM interval recorded for BLMTI.05L3.B2E10_TCLA.A5L3.B2. It shows a very linear relationship between the two offsets, with a few outliers in which the post-offset is slightly larger. The behaviour of post-offsets discussed above are the cause of these outliers.

In Figure 16, the offset measurement that has been used to correct the TID measured in each BLM interval is plotted against the time the offset interval was measured at. The ratio plot shows the offset removal methods are very similar, but that the post-offset is significantly larger for some of the intervals. An outlier can also be identified in this Figure, occurring around November. This outlier is a post-offset, and is much larger than any of its

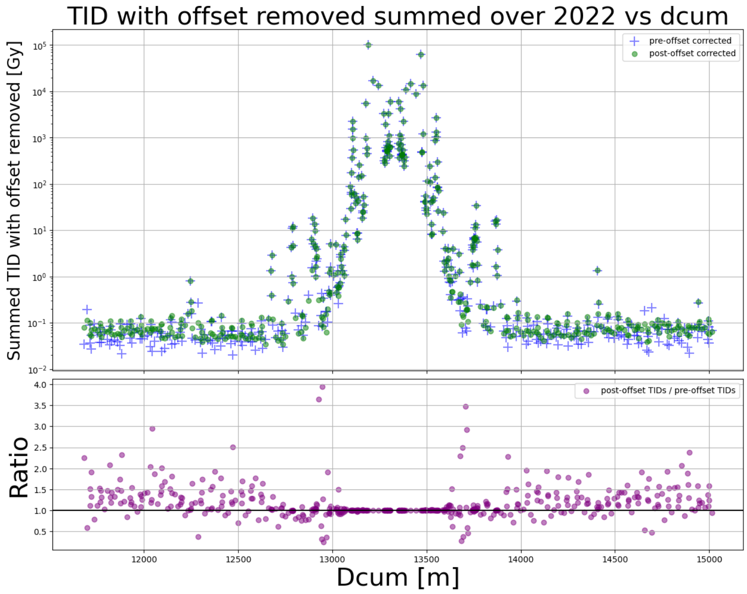

Figure 13: Total offset-corrected TID measured per BLM over 2022 against dcum for pre-offset and post-offset.

surrounding offset measurements. Analysis into this showed that the outlier was due to the post-offset including more of the decreasing beam activation than its neighbouring offsets.

4.3.3 BLMQI.01R5.B2I20_MQXA

In this section, the comparison of the pre-offset and post-offset measurements for BLMQI.01R5.B2I20_MQXA is discussed.

Figure 17 shows the pre-offset against the post-offset for every BLM interval recorded for BLMQI.01R5.B2I20_MQXA. This BLM generally has a linear relationship between the pre-offset and the post-offset. However, there are a large number of intervals in which the post-offset is significantly larger than the pre-offset, shown in the Figure by all of the outliers.

Indeed, Figure 18 shows multiple instances in which the post-offset is used, and the post-offsets are measuring much higher radiation levels than the pre-offsets. In fact, this kind of relationship was the case for the majority of the BLMs.

4.3.4 BLMQI.03L2.B2I30_MQXA

In this section, the comparison of the pre-offset and post-offset measurements for BLMQI.03L2.B2I30_MQXA is discussed.

Figure 19 shows the pre-offset against the post-offset for every BLM interval recorded for BLMQI.03L2.B2I30_MQXA. It also shows a linear relationship between the pre-offset and the post-offset. However, the figure for this BLM differs from the previous BLMs since it shows a bias towards the pre-offset, whereas previously the opposite was true. There are also three outliers for which the pre-offset is significantly larger, but also three outliers for which the post-offset is significantly larger.

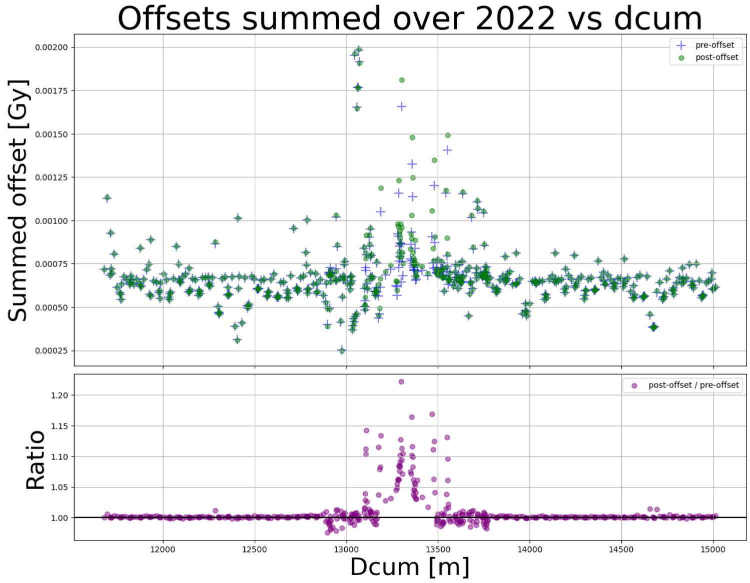

Figure 14: Total offset measured per BLM over 2022 against dcum for pre-offset and post-offset.

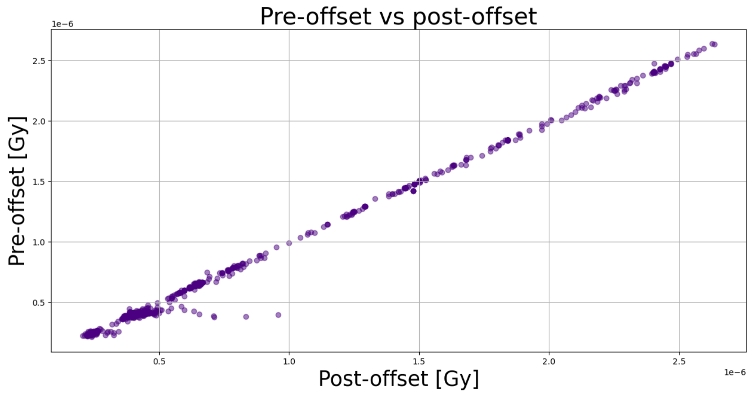

Figure 15: Post-offset against pre-offset for BLMTI.05L3.B2E10_TCLA.A5L3.B2.

The ratio plot in Figure 20 confirms that there definitely exists a bias towards the pre-offset for this BLM, since most of the points lie just below one. Analysing why this might be the case for this and other BLMs, note that the annual dose measured by this BLM was 15 Gy, whereas for BLMQI.01R5.B2I20_MQXA and BLMQI.03L2.B2I30_MQXA, their annual doses were 310 Gy and 377 Gy, respectively. Initially, one might hypothesise that a BLMs bias to offset method might correlate with the dose rate it typically measures. However, this relationship would require further analysis to confirm.

However, there are three outliers for which the post-offset is larger, and the ratio between the two for these outliers is really quite large. Looking into this, it was found that these outliers were actually due to unavailable offset measurements. As discussed in Section 2, beam intervals that are very close together result in no offset measurement being made in between these intervals. The largest outlier in the ratio plot in Figure 20 is due to a BLM intervals post-offset being larger than its pre-offset. In fact, the post-offset for the

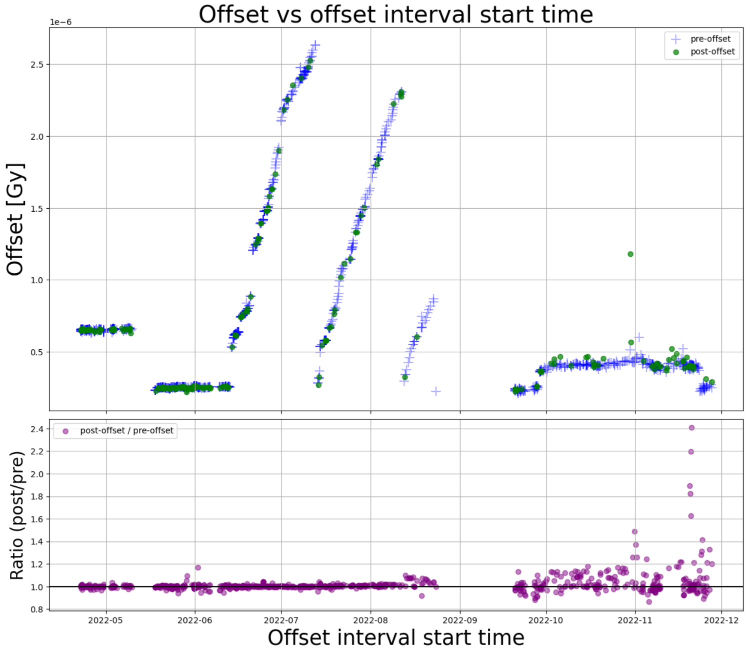

Figure 16: Offset measurements against time for BLMTI.05L3.B2E10_TCLA.A5L3.B2.

BLM interval of this outlier is actually the pre-offset of a BLM interval occurring after this interval. This can be seen in the plot showing offset against time, as the outlier we see corresponds to a pre-offset.

Analysis into why this pre-offset measurement is so large compared to its surrounding offset measurements can be seen in Figure 21. Recall from Section 2 that false spikes in radiation are recorded after fills due to BLM resets. It was discussed how the current solution rejects any offset intervals that have large fluctuations in dose rate, thereby not including these spikes in any offset measurements. This outlier is an example of when this method fails to detect a spike. The figure shows on the right the spike recorded by running sum 12, which is what has been used to produce the above figures. This spike has an abnormal behaviour such that it is very flat at its peak, and since the offset interval took place during

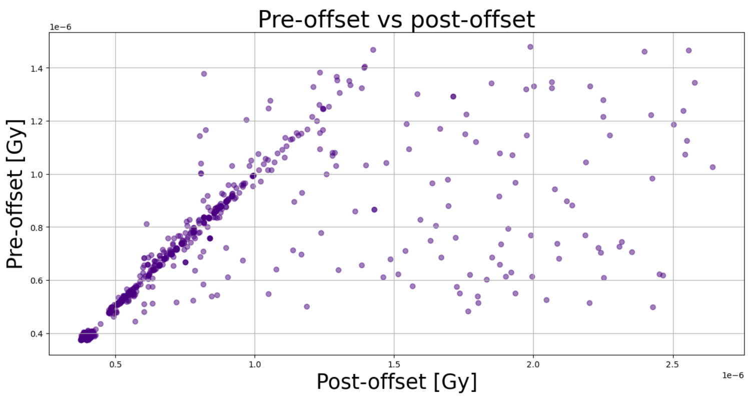

Figure 17: Post-offset against pre-offset for BLMQI.01R5.B2I20_MQXA.

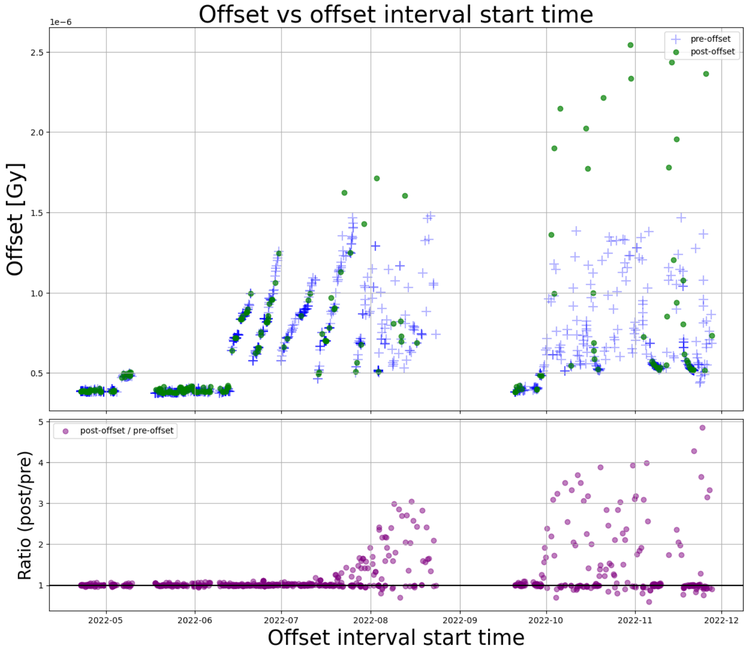

Figure 18: Offset measurements against time for BLMQI.01R5.B2I20_MQXA.

this peak, no fluctuations in dose rate were observed. Hence, the spike was not flagged. However, on the left, the spike observed by running sum 9 does indeed fluctuate. Hence, this outlier might not have been measured if running sum 9 had been in use.

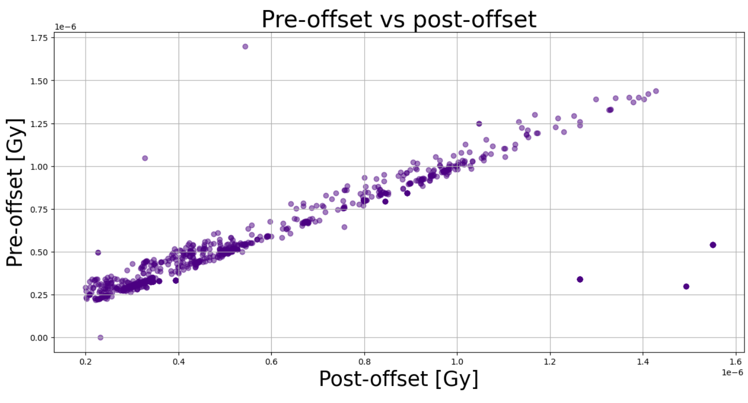

Figure 19: Post-offset against pre-offset for BLMQI.03L2.B2I30_MQXA.

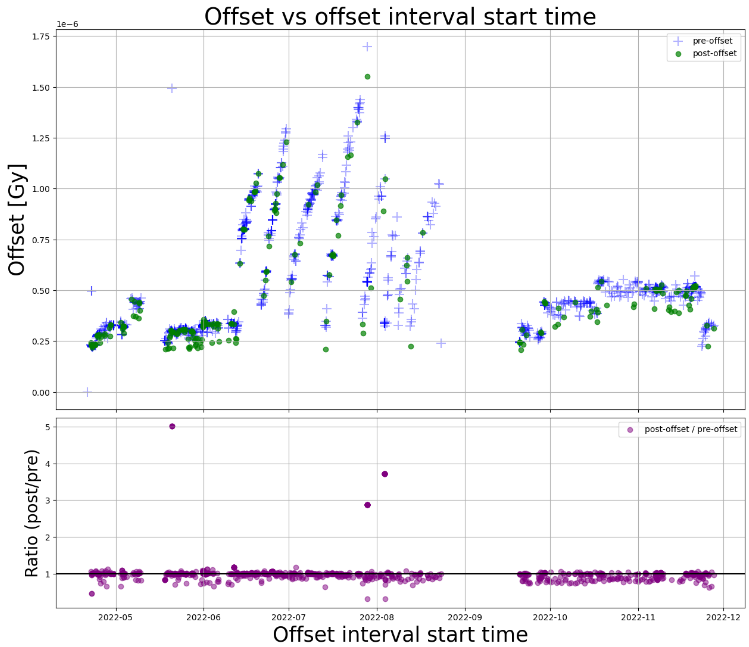

Figure 20: Offset measurements against time for BLMQI.03L2.B2I30_MQXA.

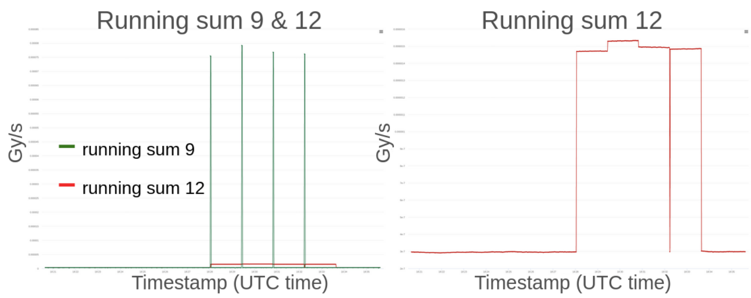

Figure 21: Offset measurement against time for BLMQI.03L2.B2I30_MQXA. The left plot shows running sum 9 and 12. The right plot shows running sum 12 only.

5 Conclusions

Overall, it has been shown that, in general, the current method and the design choices don't cause any significant problems. However, improvements can definitely be made.

When comparing running sum 9 and running sum 12, they were found to be in general very similar. However, when measuring post-offsets, running sum 12 tended to overestimate compared to running sum 9 due to decreasing beam activation still present after a beam interval. Also, BLM intervals were found for which running sum 12 failed to detect BLM reset spikes, whereas running sum 9 did not.

When comparing the method of letting the corrected TID values be negative to correcting them to zero, there was again no major differences. However, it was found that the correction to zero induces a bias at BLMs experiencing low dose rates. The correction to zero propagated into the results from analysing one year, implying that this correction is non-negligible for the low-dose BLMs. However, setting the TIDs to zero makes the results more stable and less sensitive to offset fluctuations, which could be more beneficial.

When comparing using the pre-offset and using the post-offset, it was observed that the post-offsets were generally slightly larger than the pre-offsets, again due to the decreasing beam activation being present after a beam interval. One way this could be mitigated is by measuring the post-offset slightly later, in order to reduce the impact made by the beam activation. Another option would be to instead use running sum 9, since running sum 9 sits slightly lower than running sum 12 when the radiation is decreasing. Lastly, it was found that a small proportion of BLMs actually had the opposite relationship, in that the the pre-offset tended to be larger than the post-offset. From initial observation, this could be in correlation with the typical dose rates experienced by the BLMs, but this requires further analysis.

The final conclusions are:

- Running sum 9 is preferred
- Pre-offset confirmed as best choice for offset removal
- Need to establish whether to reduce fluctuations with the zero correction or removing bias by allowing negative TIDs

References

[1] B. Dehning, E. Effinger, J. Emery, G. Ferioli, G. Guaglio, E. B. Holzer, D. Kramer, L. Ponce, V. Prieto, M. Stockner, and C. Zamantzas. The lhc beam loss measurement system. In *2007 IEEE Particle Accelerator Conference (PAC)*, pages 4192–4194, 2007.

[2] Bilko K. *Automated Analysis of the Prompt Radiation Levels in the CERN Accelerator Complex.* IPAC, 2022.